

Electrokinetic Maneuvering of Bubble-Driven Inertial Micro-Pumping Systems

Aditya Bandopadhyay¹, Uddipta Ghosh², Debashis Pal^{1,3}, Kaustav Chaudhury² and Suman Chakraborty^{1,2,*}

¹Advanced Technology Development Center, Indian Institute of Technology Kharagpur, Kharagpur - 721302, India

²Department of Mechanical Engineering, Indian Institute of Technology Kharagpur, Kharagpur - 721302, India

³Aerospace Engg. & Applied Mechanics, Indian Institute of Engineering Science and Technology Shibpur, Howrah – 711103, India

ABSTRACT

The pumping of an aqueous electrolyte by means of an asymmetrically placed thermal resistor and electrodes is investigated in this work. This device has no moving parts and provides a continuous and controllable pulsating flow, which make it a very attractive and viable option for use on lab-on-a-chip devices. The electric field induced modulation provides a higher degree of control on the mass flow rate, by means of which one can achieve on-the-fly mass flow rate control. The pumping action is achieved by means of a high-pressure bubble generated by actuating a thermal resistor which is located asymmetrically between two reservoirs. The ends of the channel are connected to fluidic columns. The combined action of an applied electric field and a faster refilling of the shorter arm after bubble collapse essentially drive a net amount of electrolyte through the system. We study the influence of the geometric parameters like the location of the heater, channel width and the channel length apart from the physiochemical parameters like the Debye length and the applied field strength on the mass flow rate achieved through this device.

1. INTRODUCTION

Modern solution to practical engineering problems involves the development of compact and smart devices, popularly known as ‘lab-on-a-chip’ technologies, which falls within the broad area of microfluidics. The wide spectrum of applicability of on-chip technologies provides us with challenges for further development towards smarter and more efficient devices [1]. One such key area for exploration is the efficient and reliable pumping of liquids at the micro-scale. Drawing parallel from thermal ink jet (TIJ) printing process, bubble-driven inertial micro-pumping mechanisms draw major attention of present day research, owing to its inherent simple *modus operandi*, ease of fabrication and on-chip integrability [2-6]. Although scores of studies have been dedicated in understanding and utilizing the inherent hydrodynamic features of the bubble-driven inertial micropumps, the possibility of additional flow control by electrokinetic effects has hitherto remained unexplored to the best of our knowledge. In the present study we, therefore, attempt to unveil the inherent attributes of electrokinetic maneuvering of bubble-driven inertial micropumps.

In microscale transport process, interfacial effects are mainly utilized for flow actuations, owing to the domination of interfacial forces over volumetric forces at such small scales. Typically, at such length scales, the inertial effects are often neglected. On the contrary, bubble driven inertial micropumps, utilize the inertial effects to bring about efficient driving of liquids through

* Corresponding author: suman@mech.iitkgp.ernet.in

microchannels. Successive generation of vapor bubbles achieved through local heating by means of a resistor, and its subsequent collapse can create favorable hydrodynamic conditions for driving liquids through the microchannel; this is the simple hydrodynamic principle that governs the operation of bubble-driven inertial micropump [2-6]. It has been previously demonstrated by Tornainen [2,3] that when a pulse of high quantity heat flux is injected into the fluid, it creates a vapor bubble, which initially increases in size, thus creating two separate columns of fluid in the channel (see figure 1). Following an initial period of volume expansion, when the heat pulse is absent, the bubble starts shrinking and eventually it collapses. During the post collapse phase, liquid fronts from two directions collide with each other. The location of this collision is asymmetric with respect to the resistor and hence subsequent momentum transfer combined with the liquid inertia drives the flow thereafter [2-6]. This characteristic makes bubble-driven inertial pumping systems, superior over other micro-pumping systems, such as electroosmotic pumping, which is employed typically for ionic solutions only. However, we must appreciate that electrokinetic driving of fluid flows in microchannels, can provide multiple possibilities of alteration in the flow fields. The fundamental of electroosmotic pumping lies in the formation of an electrical double layer (EDL) which is a distribution of coions and counterions in a solution with a specified wall potential [7]. With this motivation in mind, in this particular work we employ an externally applied electric field over an ionic aqueous solution, within which the local vapor generation-growth-collapse and subsequent post collapse pumping phenomena occurs. With this setup under consideration, we study the combined consequences of the hydrodynamics and the electrokinetics on the performance of bubble-driven inertial micro-pumping systems.

From the present analysis we reveal that during the vapour bubble generation-growth and collapse phase, the hydrodynamic features play a dominant role over the electrokinetic effects. We demonstrate that during the post collapse phase, a high degree of flow control is possible by the changing the direction and magnitude of the applied electric field.

2. MATHEMATICAL FORMULATION

As a physical system for the present study, we consider a 2-dimensional rectangular channel of height $2H$ and length L , as depicted in figure 1.

The whole channel is initially filled with liquid, with a small heater placed asymmetrically on the bottom wall. The two ends of the channel are at distances L_1 and L_2 from the heater and we denote the two sides of the heater as arms. We will assume $L_2 > L_1$ and hence will call the arm on the left side

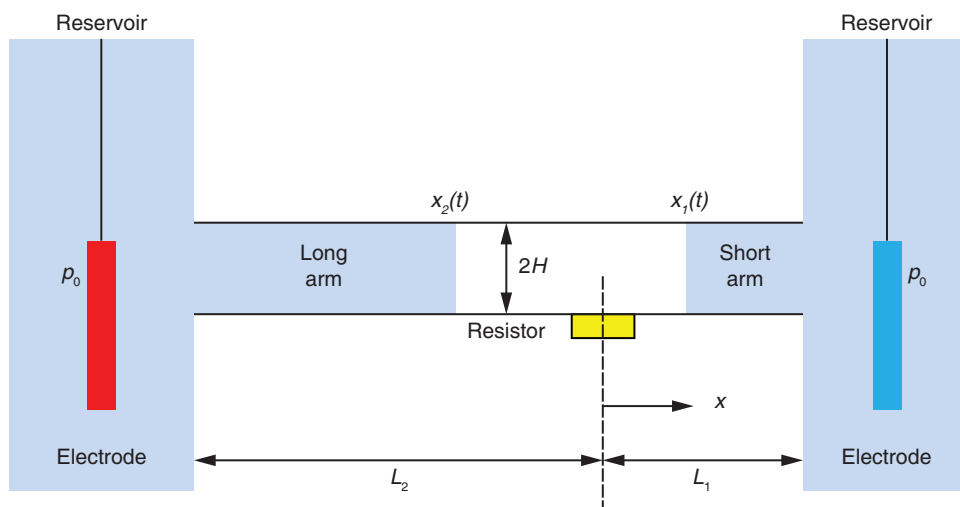


Figure 1. A Schematic description of the problem

(please refer to figure 1) as the long arm and that on the right hand side to be the short arm. We note that $L = L_1 + L_2$. We denote the ratio $L_2/(L_1 + L_2)$ by R which is a measure of asymmetry of the heater location. In addition to the heater, two electrodes are also placed at the two ends of the channel, with a voltage V_0 being applied between them. The fluid in the channel bears some electrolytes (for e.g. KCl) and the channel walls are assumed to bear a surface charge, which we express as equivalent surface or zeta potential, given by ζ [7]. The two ends of the channel are considered to be at the same pressure (atmospheric pressure, p_0), which can be achieved by connecting the channel to two large reservoirs. We place the origin on the heater, where the x axis runs along the channel and the y axis runs vertically. Here, we note that our system resembles the one previously described by Tornaiainen et al [2,3] regarding their work with bubble-driven inertial micro-pumps.

Now, we briefly mention the working mechanism of the pump. At $t = 0$, the heater is switched on for a short period of time (say τ), during which it provides the liquid with very high amount of concentrated heat flux. Absorbing this heat, the fluid near the heater vaporizes and creates a bubble, which initially expands at a rapid pace and separates two columns of liquids in the short and the long arm. After the heater is switched off, the bubble slowly starts to shrink and eventually the liquid columns meet. However, owing to the asymmetry in the position of the heater, the two columns would not meet exactly on the heater, which indicates that there will be a net momentum of the total liquid body after the collision. This will create a net flow in the channel [2-6]. In the present case the shorter arm will have higher momentum and hence the flow will be from right to left, i.e., in the negative x direction. A more detailed mechanism for the working principle of such pumps can be found in the work by Tornaiainen et al [2,3], Yuan and Prosperetti [4] and Yin and Prosperetti [5,6]. At this stage the presence of the external electric field along with electrical charges in the solution, will create an additional driving force in the liquid, which might aid or oppose the momentum imparted to the fluid by the bubble collapse, depending on the direction of the electric field and the sign of the surface potential [7].

In an effort to write the equations for fluid motion, we adapt the lumped approach [2-6]. Here, we note that for the initial instants, i.e., when the heater is on, the difference between the vapour pressure inside the bubble and the reservoir pressure remains high and hence the liquid columns are primarily driven by this pressure difference. Therefore, for the time span $0 < t < \tau$, we can safely neglect the contributions from the electrical forces. Denoting the position of the left end of the bubble by x_2 and that of the right end by x_1 , we write the equation of motion for the two arms, in the following way [2-6]:

$$\rho A(L_1 - x_1)\ddot{x}_1 + \kappa(L_1 - x_1)\dot{x}_1 = (p_v - p_0)A - 4\sigma A / D_h \quad (1.a)$$

$$\rho A(L_2 + x_2)\ddot{x}_2 + \kappa(L_2 + x_2)\dot{x}_2 = (p_0 - p_v)A + 4\sigma A / D_h \quad (1.b)$$

Here, \dot{x} denotes $\frac{dx}{dt}$ and so on. In equations (1.a) and (1.b), σ is the surface tension between the liquid and the vapour, A is the cross sectional area of the channel, D_h is the hydraulic diameter of the channel, κ is a constant which denotes the strength of the viscous drag force on the fluids and ρ is the density of the fluid. Equations (1.a) and (1.b) are simple momentum balance equations, obtained by taking into account various forces acting on the liquid columns. Note that these equations are only valid for the time span $0 < t < \tau$. For $t > \tau$, since the heater is switched off, we have to take into account the electrical body forces acting on the liquid column. The electrical body forces are simply evaluated by multiplying the total charges present in the solution with the axial electric field [7]. The charge distribution in the liquid is given by the Poisson-Boltzmann equation, with Debye-Huckel linearization, expressed as: $\frac{d^2\psi}{dy^2} = \frac{\psi}{\lambda^2}$, where, λ is the Debye length expressed as: $\lambda^{-2} = \frac{2n_0z^2e^2}{\epsilon_l kT}$ (ϵ_l is the permittivity of the liquid, k is the Boltzmann constant, T is the temperature, n_0 is the bulk electrolyte density, z is the valance of the ions and e is the electron charge). The aforementioned equation is solved with the boundary conditions, $\psi(2H) = \psi(0) = \zeta$, which gives the solution, $\psi = \zeta \cosh [H-y]/\lambda / \cosh (H/\lambda)$ [7]. The

charge density is obtained from the Poisson equation. Employing the derived potential distribution, the charge density is of the form [7]:

$$\rho_e = -\frac{\varepsilon \zeta \cosh[(H-y)/\lambda]}{\lambda^2 \cosh(H/\lambda)} \quad (2)$$

The electric fields (axially applied) satisfy the following equations [7]: (a) Continuity of displacement field, $\varepsilon_l E_l = \varepsilon_l E_2 = \varepsilon_v E_v$ and (b) the total potential drop, $E_2(L_2 + x_2) + E_v(x_1 - x_2) + E_1(L_1 - x_1) = V_0$, where E_1 and E_2 are the electric fields in the short and the long arms respectively and E_v is the electric field inside the bubble. Solving these equations, one obtains the electric fields in the liquid columns as:

$$E_1 = E_2 = \frac{L}{L + (x_1 - x_2)(\varepsilon_r - 1)} \quad (3)$$

Here, $\varepsilon_r = \varepsilon_l / \varepsilon_v$. Therefore, the body force can be calculated from the relation: $F_e = \int_0^L \int_0^{2H} \rho_e E dy dx$. Putting the charge distributions in this equation, we get the forces acting on different arms as follows (width is chosen to be w):

$$\text{Short arm: } F_{e,1} = -\frac{2w\varepsilon_l \zeta (L_1 - x_1) \tanh(H/\lambda) E_1}{\lambda} \quad (4.a)$$

$$\text{Long arm: } F_{e,2} = -\frac{2w\varepsilon_l \zeta (L_2 + x_2) \tanh(H/\lambda) E_2}{\lambda} \quad (4.b)$$

Now, we can write the equation of the motion for the two liquid columns after time $t > \tau$, by incorporating the body forces in the momentum equation. The equations are given by:

$$\begin{aligned} & \rho A (L_1 - x_1) \ddot{x}_1 + \kappa (L_1 - x_1) \dot{x}_1 \\ & = (p_v - p_0) A - 4\sigma A / D_h - \frac{2w\varepsilon_l \zeta (L_1 - x_1) \tanh(H/\lambda) E_1}{\lambda} \end{aligned} \quad (5.a)$$

$$\begin{aligned} & \rho A (L_2 + x_2) \ddot{x}_2 + \kappa (L_2 + x_2) \dot{x}_2 \\ & = (p_0 - p_v) A + 4\frac{\sigma A}{D_h} - \frac{2w\varepsilon_l \zeta (L_2 + x_2) \tanh(H/\lambda) E_2}{\lambda} \end{aligned} \quad (5.b)$$

Thus equations (1.a) and (1.b) for $0 < t < \tau$ and (5.a – 5.b) for $t > \tau$ with the initial conditions $x_1(0) = \dot{x}_1(0) = 0$ and $x_2(0) = \dot{x}_2(0) = 0$ gives the complete account of the liquid column motion before the bubble collapse. After the columns merge, we have to account for only a single liquid body from that time onwards. We denote the motion of the liquid after collision, by tracking the evolution of the collision point with time ($x(t)$). At this stage the mass of the column becomes constant at $\rho A(L_1 + L_2)$ and the magnitude of the electric field acting on the liquid body also becomes constant at $E = V_0/L$. The equation of motion is described simply as [2-6]:

$$\rho A L \ddot{x} + \kappa L \dot{x} + \frac{2w\varepsilon_l E \zeta L \tanh(H/\lambda)}{\lambda} = 0 \quad (6)$$

The initial conditions for equation (6) is given by, $x(t_c) = x_1(t_c) = x_2(t_c)$, where t_c is the time of collision. The velocity of the collision point is obtained by applying conservation of momentum at time $t = t_c$ (since there is no impulse force acting on the liquid columns during the collision). The equation for conservation of momentum reads $\rho A(L_1 - x_1)\dot{x}_1 + \rho A(L_1 + x_2)\dot{x}_2 = \rho A L \dot{x}$, which makes the other

initial condition for the equation (6) to be: $\dot{x}(t_c) = \frac{(L_1 - x_1)\dot{x}_1(t_c) + (L_2 + x_2)\dot{x}_2(t_c)}{L}$. Equations

(1) ($0 < t < \tau$), (5) ($\tau < t < t_c$) and (6) ($t > t_c$), along with the pertinent initial conditions, represents the complete dynamics of the liquid in the channel. Note that t_c is not known a-priori and has to be calculated from the solutions of equations (1) and (5), using the matching condition $x_2 = x_1$ at $t = t_c$. The volume throughput is given by the expression: $Q = A x(t_f)$ where t_f is the final time [2,3]. Next we aim to non-dimensionalize the pertinent equations. Towards this, we chose the following scales for non-dimensional variables:

$\bar{x} = x / D_h$; $\bar{t} = t / \tau$; $\bar{E} = E / (V_{ref} / L)$; $\bar{p} = p / p_v$; $\bar{\lambda} = \lambda / D_h$; $\bar{L} = L / D_h$ (L can be any length scale and V_{ref} is a fixed reference voltage). The non-dimensional equations are finally written as:

For $0 < \bar{t} < 1$:

$$\begin{aligned} \text{Arm 1: } & (\bar{L}_1 - \bar{x}_1)\ddot{\bar{x}}_1 + \alpha(\bar{L}_1 - \bar{x}_1)\dot{\bar{x}}_1 \\ & = \beta(p_v - p_0) / p_v - 4\gamma \end{aligned} \quad (7.a)$$

$$\begin{aligned} \text{Arm 2: } & (\bar{L}_2 + \bar{x}_2)\ddot{\bar{x}}_2 + \alpha(\bar{L}_2 + \bar{x}_2)\dot{\bar{x}}_2 \\ & = \beta(p_v - p_0) / p_v + 4\gamma \end{aligned} \quad (7.b)$$

For $1 < \bar{t} < \bar{t}_c$:

$$\begin{aligned} \text{Arm 1: } & (\bar{L}_1 - \bar{x}_1)\ddot{\bar{x}}_1 + \alpha(\bar{L}_1 - \bar{x}_1)\dot{\bar{x}}_1 \\ & = \beta(p_v - p_0) / p_v - 4\gamma - \xi \tanh(\bar{H} / \bar{\lambda}) \bar{E}_1 (\bar{L}_1 - \bar{x}_1) \end{aligned} \quad (7.c)$$

$$\begin{aligned} \text{Arm 2: } & (\bar{L}_2 + \bar{x}_2)\ddot{\bar{x}}_2 + \alpha(\bar{L}_2 + \bar{x}_2)\dot{\bar{x}}_2 \\ & = \beta(p_v - p_0) / p_v + 4\gamma - \xi \tanh(\bar{H} / \bar{\lambda}) \bar{E}_2 (\bar{L}_2 + \bar{x}_2) \end{aligned} \quad (7.d)$$

For $\bar{t} > \bar{t}_c$:

$$\ddot{\bar{x}} + \alpha\dot{\bar{x}} + \xi \tanh(\bar{H} / \bar{\lambda}) \bar{E} \bar{L} = 0 \quad (7.e).$$

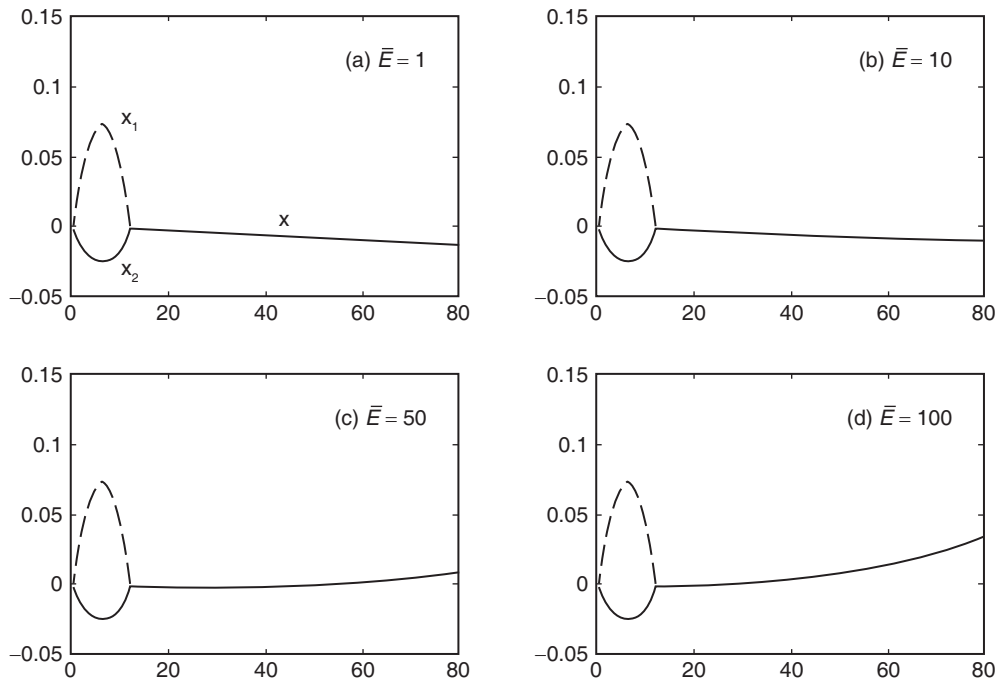
In equation set (7), the various parameters are given by $\alpha = \kappa\tau / \rho A$, $\beta = p_v \tau^2 / \rho D_h^2$, $\gamma = \sigma \tau^2 / \rho D_h^3$, and $\xi = \Omega / \bar{\lambda} \text{Re}$, where $\Omega = u_{HS} / u_{ref}$, $\text{Re} = \rho H u_{ref} / \eta$. Here, u_{HS} is the Helmholtz-Smoluchowski velocity, given by, $u_{HS} = -\epsilon_l \zeta E_{ref} / \eta$ [7] and u_{ref} is the reference velocity, given by: $u_{ref} = D_h / \tau$. The above set of equations has been numerically solved using a fourth order Runge-Kutta method in MATLAB. In the next section we describe the pertinent results obtained from the solutions.

3. RESULTS AND DISCUSSIONS

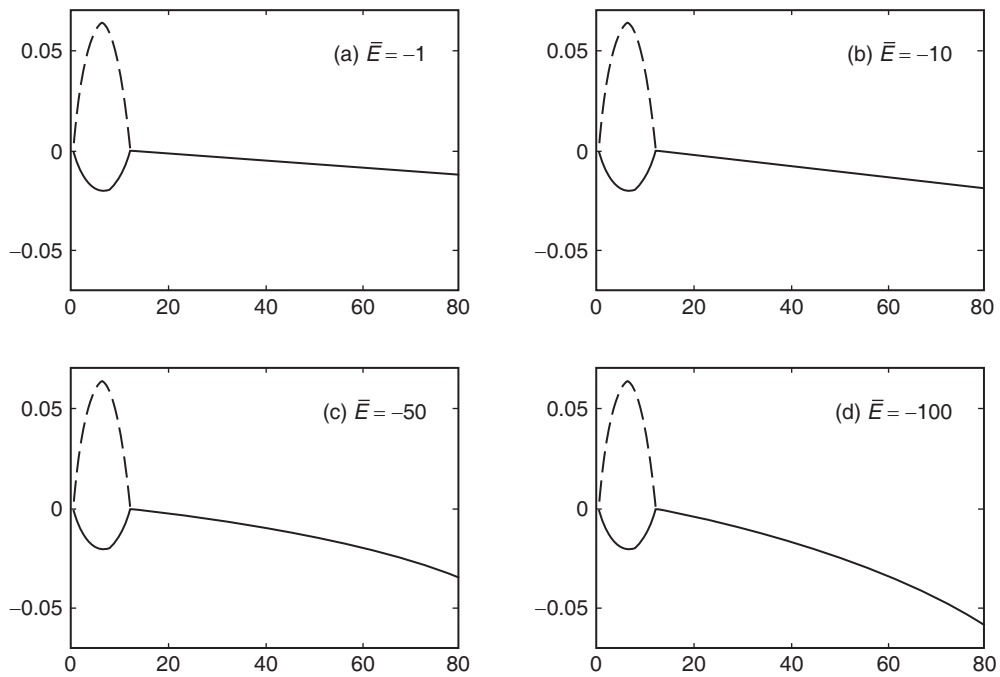
In an effort to represent our results, we have chosen the following values of the relevant parameters [2, 3]: $D_h = 100 \mu\text{m}$, $\kappa = 50 \text{ cP}$, $p_0 = 1 \text{ atm}$, $p_v = 7 \text{ atm}$, $\tau = 1 \mu\text{s}$, $\zeta = -25 \text{ mV}$, $E_{ref} \sim 10^4 \text{ V/m}$, $\sigma = 0.1 \text{ N/m}$, $\rho = 1000 \text{ kg/m}^3$, $\epsilon_l = 80\epsilon_0$ (ϵ_0 is the permittivity of vacuum) and $\bar{L} = 10$. Unless otherwise mentioned, the value of R has been taken as 0.75.

For understanding the operation of a bubble-driven inertial micropump, it is customary to investigate movements of the fronts of the liquid columns (x_1 , x_2 and x), as shown in the figure 2.

Here we demonstrate the front movement for different strengths of applied electric fields (\bar{E}). As per our notion of a negligible contribution of electric field during the bubble formation-growth-collapse regime, one can identify the prominent effect of electric field in the post collapse regime. Note that a monotonous flow rate with a downwards slope indicates that the flow is being aided by the electric field whereas an upwards



(a) Positive electric field: opposes the flow



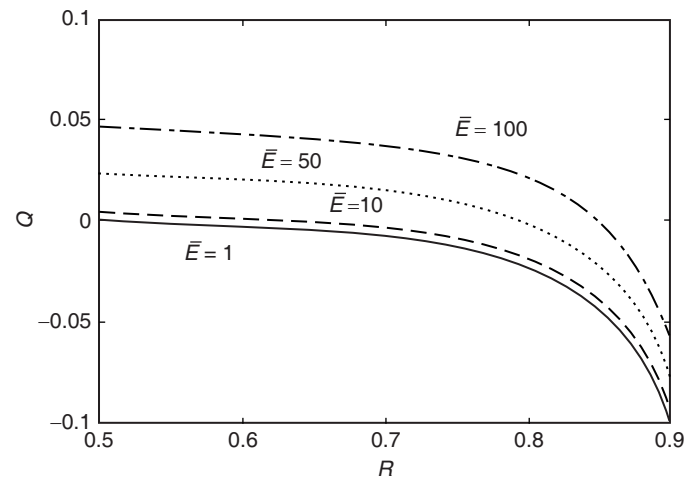
(b) Negative electric field: aids the flow

Figure 2. Variation of x (position) as a function of t (time) for different applied electric fields. same line-style notions are followed for all the figures

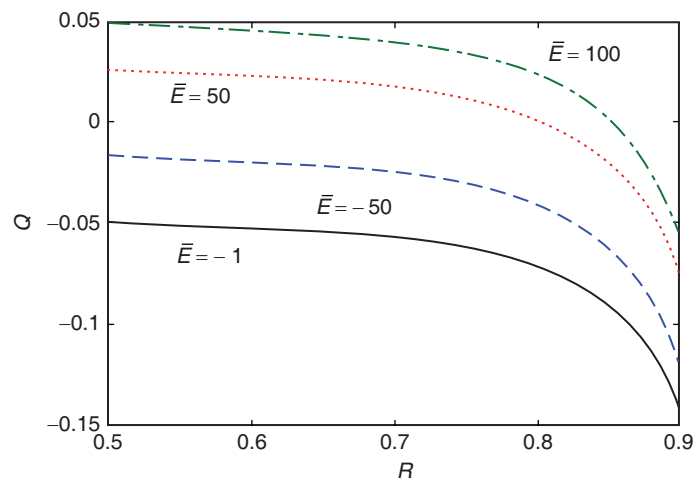
slope indicates that the flow is being opposed by the electric field. Since the pumping action of the system, specifically in the post collapse regime, is governed by the inertia of the incipient liquid medium, the electric field endorses an additional body force that provides further maneuverability. In absence of any electric field, the liquid element at the collapsing point shows a tendency to move towards the long arm. This feature is clearly seen in the present study when the magnitude of \bar{E} is low. However, with an increase in the strength of the electric field, the directional preference to movement can be completely reversed (compare the case for $\bar{E} = 50$ and 100). Moreover, in tune with aiding, one can obtain enhanced maneuverability for a reversed polarity (compare the case for $\bar{E} = -50$ and -100).

We now evaluate the performance of the pumping system in terms of its flow rate characteristics. In tune with the popular notion of demonstrating flow rate alteration due to different resistor locations(R), here we demonstrate a finer control of the flow rate by the application of electric field, as is shown in the figure 3.

As per our previous discussion, in connection to figure 2, we can obtain altered flow direction over a wide range of resistor location (compare the case for $\bar{E} = 50$ and 100). Moreover, one can appreciate



(a) Cases of positive (opposing) electric field



(b) Cases of negative (aiding) as well as positive (opposing) electric field

Figure 3. Variation of the volume throughput as a function of the resistor location for different applied electric fields

that at any location of the resistor, it is possible to obtain zero or no-flow rate condition by application of electric field of suitable strength. Thus, one of the major advantages with electrical manipulation that one can obtain an on-the-fly zero flow rate as and when required. Moreover, when it comes to providing controlled flow rate, normal bubble-driven inertial micropumps rely on shifting the resistor location, which is a daunting task post-fabrication. However, with electrical manipulation, one may set the resistor location once and obtain controlled flow rate just by changing the direction and magnitude of strength of applied electric field. While accounting for the electrokinetic effects, it is important to study the electrokinetic parameters underpinning the physical processes. As already discussed, the surface electrochemistry dictates the development of electric potential over the wall of the channel (characterized by zeta potential). In such cases, the velocity is typically characterized as the *Helmholtz-Smoluchowski velocity* [7]. Encompassing these factors, we have already defined a parameter called dimensionless surface potential(ξ).

In figure 4 we plot variation of the flow rate with ξ at different resistor locations. It is evident that inertia dominated flow generates negative Q . As the magnitude of ξ increases, electroosmotic component of Q becomes stronger and the volume throughput tends to become more and more positive (for a given positive applied electric field). Thus, one may also exploit the intricate surface electrochemistry to advantageously control the flow behavior. Such characterization, as we expect, is critical for choosing an appropriate substrate-electrolyte pair for design of futuristic pumping devices.

We explore the effects of penetration of the electrical double layer as compared to the channel height. Towards this, we plot the variation of the flow rate as a function of the dimensionless Debye length for different strength of applied electric field in figure 5. This knowledge is crucial to account for the concentration of the electrolytes in the solution. It can be seen from figure 5 that as λ is increased, the magnitude of volume flow rate decreases. A larger λ is indicative of a much larger EDL in comparison with the channel height. In such cases the EDL potential distribution will change and hence the “effective” electroosmotic velocity. Thus, the electroosmotic component of flow will decrease, and Q becomes more and more negative.

4. CONCLUSIONS

In the present analysis, we have successfully demonstrated that the flow rate in a bubble-driven inertial pump can be controlled intricately by using an electrolyte solution in conjunction with externally applied electric field. We have shown that the displacement of the collapse point depends strongly on the direction of the applied electric field as well as the sign of the surface or zeta potential. For the

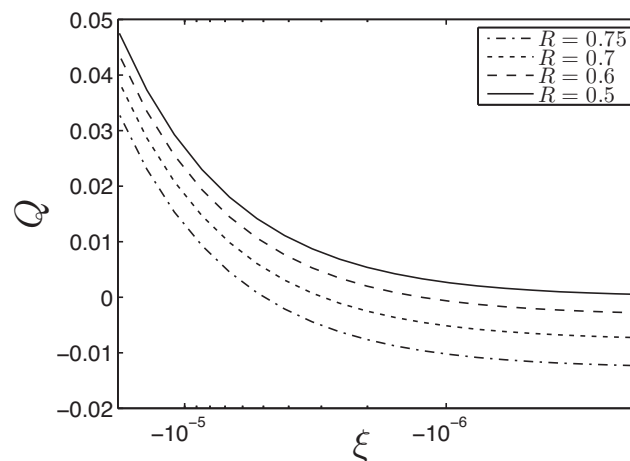


Figure 4. Plot of volume throughput with the parameter ξ , for different positions of the heater, as denoted by R

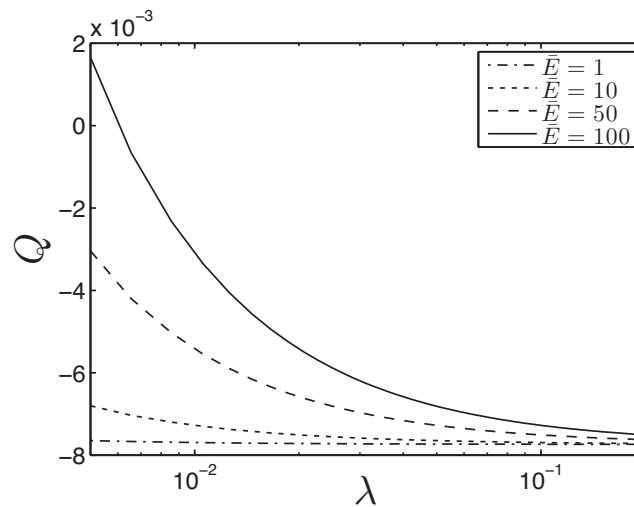


Figure 5. Plot of volume throughput with dimensionless Debye length, for different strengths of the applied electric field

specific sign of the surface potential used here, we observe from the present analysis that a negative electric field greatly augments the throughput, whereas a positive electric subdues the motion generated from the collapse of the bubble. We additionally depict that the flow rate increases with increasing R , i.e., increasing asymmetry. An increase in the thickness of the EDL, however, reduces the net throughput. We further observe from the present analysis that, the net throughput can be in both the directions, when we apply strong enough electric fields in the channel. Therefore, in essence, we can conclude that the application of external electric field in bubble-driven inertial micropump gives us a greater controllability over the net throughput, bearing far ranging scientific and technical implications in the area of miniaturized devices.

REFERENCES

- [1] R. B. Schoch, J. Han and R. Renaud, Transport Phenomena in nanofluidics, *Reviews of Modern Physics*, 2008, 80(3) pp 839–883.
- [2] P. E. Kornilovitch, A. N. Govyadinov, D. P. Markel and E. D. Torniainen, One-dimensional model of inertial pumping, *Physical Review E*, 2013, 87(2) pp 023012–023023.
- [3] E. D. Torniainen, A. N. Govyadinov, D. P. Markel and P. E. Kornilovitch, Bubble-driven inertial micropump, *Physics of Fluids*, 2012, 24(12) pp 122003–122020.
- [4] H. Yuan, and A. Prosperetti, The pumping effect of growing and collapsing bubbles in a tube, *Journal of Micromechanics and Mircoengineering*, 1999, 9(4) p. 402
- [5] Z. Yin, and A. Prosperetti, A microfluidic ‘blinking bubble’ pump, *Journal of Micromechanics and Mircoengineering*, 2005, 15(3) p 643
- [6] Z. Yin, and A. Prosperetti, ‘Blinking bubble’ micropump with microfabricated heaters, *Journal of Micromechanics and Mircoengineering*, 2005, 15(9) p 1683
- [7] R. J. Hunter, *Zeta potential in colloidal science*, 1981, Academic Press, London.

